Journal of Molecular Catalysis A: Chemical 385 (2014) 125–132

Contents lists available at ScienceDirect

Journal of Molecular Catalysis A: Chemical

journal homepage: www.elsevier.com/locate/molcata

Insights into the deactivation mechanism of supported tungsten hydride on alumina (W-H/Al_2O_3) catalyst for the direct conversion of ethylene to propylene

Etienne Mazoyer[a], Kai C. Szeto[a], Nicolas Merle[a], Jean Thivolle-Cazat[a], Olivier Boyron[a], Jean-Marie Basset[a,1], Christopher P. Nicholas[b,*], Mostafa Taoufik[a,*]

[a] Université Lyon 1, C2P2, CNRS UMR 5265, ICL, CPE Lyon, 43 Bd du 11 Novembre 1918, 69616 Villeurbanne, France
[b] Exploratory Catalysis Research, UOP LLC, A Honeywell Company, 25 East Algonquin Road, Des Plaines, IL 60017, USA

ARTICLE INFO

Article history:
Received 9 August 2013
Received in revised form 26 January 2014
Accepted 27 January 2014
Available online 3 February 2014

Keywords:
Heterogeneous catalysis
TGA/DSC
Solid state NMR
Polymerization
Catalyst deactivation

ABSTRACT

Tungsten hydride supported on alumina prepared by the surface organometallic chemistry method is an active precursor for the direct conversion of ethylene to propylene at low temperature and pressure. An extensive contact time study revealed that the dimerization of ethylene to 1-butene is the primary and also the rate limiting step. The catalytic cycle further involves isomerization of 1-butene to 2-butene, followed by cross-metathesis of ethylene and 2-butene to yield propylene with high selectivity. The deactivation mechanism of this reaction has been investigated. The used catalyst was extensively examined by DRIFTS, solid-state NMR, EPR, UV–Vis, TGA and DSC techniques. It was found that a large amount of carbonaceous species, which were due to side reaction like olefin polymerization took place with time on stream, significantly hindering the dimerization of ethylene to 1-butene and therefore the production of propylene.

1. Introduction

The consumption of propylene has constantly increased during the last past years. The reason is directly linked to the high demand of propylene-derived products, like polypropylene, propylene oxide and acrylonitrile [1,2]. Hence, on-purpose propylene production has become more important in addition to classical cracking methods. These approaches include propane dehydrogenation [3–5], olefin metathesis [6–11], methanol to olefins [12,13] and methyl halides to olefins [14–16]. Currently, intensive research efforts are focused on shale gas extraction, with the aim to utilize this gas as the next generation feedstock for petroleum products. The ethane content of shale gas can be up to 16%, the rest is mainly methane like natural gas. Therefore, much of the additional steam cracking capacity built in the near future will be based on using ethane as a feedstock, which typically produces only ethylene as a final product [17]. In this context, a new process that allows the selective conversion of ethylene to propylene will be economically relevant.

The conversion of three molecules of ethylene to two molecules of propylene, as presented in Scheme 1, is highly thermodynamically favored. Below 900 K the standard Gibbs free energy is negative, affording a large conversion of ethylene at equilibrium. Moreover, under 600 K, the conversion of ethylene is complete at the equilibrium (Fig. S1). Only few examples of the direct transformation of ethylene into propylene have been reported. For instance, a deficiency of ethylene formation compared to butenes has been observed during the metathesis of propylene catalyzed by [$Mo(CO)_6$]/Al_2O_3 and attributed to the direct transformation of ethylene into propylene [18]. This reaction has also been observed, with a short lifetime, during Fischer–Tropsch synthesis in the presence of small iron nanoclusters formed by the thermal decomposition of [$HFe_3(CO)_{11}$]/MgO [19]. Other reported catalysts for the transformation of ethylene to propylene are based on europium or ytterbium deposited on coal in combination with titanium compounds ($TiCl_4$, $Ti(OiPr)_4$) [20] as well as with WO_3 on various oxides [21] MoO_x/SiO_2 [22] or

* Corresponding authors at: Université Lyon 1, C2P2, CNRS UMR 5265, ICL, 43 Bd du 11 Novembre 1918, 69616 Villeurbanne, France; Exploratory Catalysis Research, UOP LLC, A Honeywell Company, 25 East Algonquin Road, Des Plaines, IL 60017, USA. Fax: +33 472431795/1 8473911287.
E-mail addresses: Christopher.Nicholas@Honeywell.com (C.P. Nicholas), mostafa.taoufik@univ-lyon1.fr (M. Taoufik).
[1] Current address: KCC, 4700 King Abdullah University of Science and Technology, Thuwal 23955-6900, Saudi Arabia.

1381-1169/$ – see front matter.
http://dx.doi.org/10.1016/j.molcata.2014.01.025

Scheme 1. Reaction of direct conversion of ethylene to propylene.

Ru/SiO catalysts [23]. However, the catalytic performances of all these systems were either not quantified or proven to be very low as they were only observed in closed recirculation systems.

A significant example of direct conversion of ethylene to propylene in terms of selectivity and productivity is reported using zeolites [24]. During their investigation, Oikawa et al. shed light upon the importance of the pore size and the acidity of the catalyst to obtain a good selectivity and conversion, respectively. They have identified SAPO-34 as the most efficient catalyst for direct ethylene to propylene conversion. Its pore size is similar to the kinetic diameter of the propylene, giving thus a good selectivity in this molecule, and its acid strength is intermediate, affording the best conversion rate. When the reaction is performed at 450 °C, after 1 h on stream, a propylene production rate of 7.00 $mmol_{C_3H_6}\ g^{-1}\ h^{-1}$ (79% selectivity) is obtained. Another example of direct conversion of ethylene to propylene has been described using nickel catalyst supported on mesoporous silica [25,26]. In that example the catalyst shows a constant activity at 400 °C, during 10 h on stream, with a propylene production of 1.85 $mmol_{C_3H_6}\ g^{-1}\ h^{-1}$ and a poor selectivity of 49%. The explanation was given by a mechanism in which ethylene dimerization on Ni sites affords 1-butene that can be isomerized to 2-butene on acidic sites. 2-Butene is supposed to react *via* cross-metathesis reaction with non-reacted ethylene. Iwamoto claims that Ni(I) are able to perform metathesis reaction by the formation of a nickel carbene (Ni(III)) intermediate. The large pore size of MCM-41 is the major argument presented to exclude an acidic mechanism such as that presented for SAPO-34. Nevertheless, after calcination of impregnated nickel nitrate, it can be agreed that the surface of the catalyst will exhibit silicates with non-negligible acidity and the high temperature of reaction does not exclude cracking of higher olefin to provide propylene as observed by Oikawa et al. These reported catalysts require high working temperature (>400 °C) to complete the classic acid catalytic cycle and will inevitably undergo rapid catalyst deactivation by formation of coke. An ultimate system will be a catalyst that works at low temperature and gives high selectivity in propylene. Our laboratory has been working extensively to develop alternative methods to produce propylene by using alkene metathesis reactions [27–31]. In this context, we recently discovered a new catalytic reaction which transforms ethylene directly to propylene at low temperature and pressure (150 °C, 1 bar) with a selectivity higher than 95% [29]. This reaction is catalyzed by tungsten hydride supported on alumina dehydroxylated at 500 °C, described elsewhere [32]. The initial postulated mechanism for the productivity of propylene involves: (i) ethylene dimerization to 1-butene; (ii) 1-butene isomerization to 2-butenes; (iii) cross metathesis between ethylene and 2-butenes. In this account, we report in details the performance of this catalyst for direct conversion of ethylene to propylene. The complete mechanism of this reaction was studied by identification of the products released in early stage of catalysts and influence of contact time. However, the tungsten hydride on alumina catalyst used here undergoes catalyst deactivation with time on stream. For further application in industry, the deactivation of the catalyst needs to be understood in order to find ways to improve the stability of the catalyst. Therefore, on-stream deactivation during conversion of ethylene to propylene over tungsten hydride catalyst was examined. TGA, DSC, solid state NMR, DRIFTS, EPR and UV–Vis techniques were used to characterize the nature of the deactivated catalyst.

2. Experimental

2.1. Catalyst preparation

The catalyst ($\mathbf{WH_3/Al_2O_{3-(500)}}$) was prepared according to published procedure reported elsewhere [32] and consisted of two steps, grafting and hydrogenolysis. The γ-alumina (Rhone-Poulenc, 200 $m^2\ g^{-1}$, XRD shown in Fig. S2) was dehydroxylated at 500 °C prior to the grafting reaction. Then, $W(\equiv CC(CH_3)_3)(CH_2C(CH_3)_3)_3$ [33] was contacted with the γ-alumina at 66 °C under argon to obtain a well-defined $W(\equiv CC(CH_3)_3)(CH_2C(CH_3)_3)_2$ fragment on the surface. Excess of the molecular complex was washed off with dry pentane and the solid was dried under high vacuum. The second step comprised a treatment of the latter solid under H_2 at 150 °C. The catalyst was then stored at −25 °C in the glove box.

2.2. Characterization

Infrared spectra were recorded in Nicolet FTIR 6700 spectrophotometer in diffuse reflectance mode, equipped with a MCT detector. Typically 64 scans with a resolution of 4 cm^{-1} were applied for each spectrum. An air-tight cell with CaF_2 window was employed. UV–vis spectra of the samples were recorded in a diffuse reflectance mode with a Perkin Elmer λ-1050 spectrometer at room temperature in the range of 200–900 nm at a rate of 275 nm min^{-1} and InGaAs detector. Electron paramagnetic resonance (EPR) experiments were performed on a Bruker EXELSYS spectrometer at room temperature. A microwave frequency ν of 9.813 GHz and a power of 30 mW were used. The reactor cell for EPR measurements was made of quartz (4 mm i.d.) and was normally charged with 0.01 g samples. Thermogravimetric analysis (TGA) was performed using a Mettler Toledo instrument TGA/DSC1. About 10 mg of sample was accurately weighed in aluminium oxide pans and heated from 35 °C to 800 °C at a rate of 20 °C min^{-1}. Air at a flow rate of 30 mL min^{-1} was used as the carrier gas. Differential scanning calorimetry (DSC) analysis was performed using a Mettler Toledo DSC 1 instrument, equipped with an auto-sampler. The temperature, the heat flow and the tau lag of the equipment were calibrated with H_2O, an indium standard and a zinc standard. The sample was accurately weighed (around 20 mg) and heated from 40 °C to 160 °C at 10 °C min^{-1} with an empty aluminum pan as reference. Two successive heating and cooling were performed and only the second run was considered. Dry nitrogen with a flow rate set at 30 mL min^{-1} was used as the purge gas. The melting temperature (Tm) was measured at the top of the endothermic peak. The STARe thermal analysis software was used to performed calculation on TGA and DSC data. ^{13}C CP-MAS solid state NMR spectra were collected on a Bruker NMR AVANCE 500 spectrometer. The sample was filled in a zirconia impeller of 4 mm and then transferred into the probe with a rotation speed of 10 kHz. Elemental analysis was performed at the Central Analysis Service of the CNRS (Solaize, France) to determine the tungsten loading (found: 5.5 wt% W).

2.3. Catalyst evaluation

Catalytic performance in ethylene conversion was assessed in a stainless steel continuous flow reactor ($P_{C_2H_4} = 1$ bar, $T = 150$ °C, flow rate = 4 mL min^{-1} or VHSV = 400 h^{-1}). The gases were purified with a column of molecular sieve and activated Cu_2O/Al_2O_3 and controlled by Brooks mass flow controllers. The catalyst was charged in the glovebox. A 4-way valve allowed isolation of the charged catalyst in the reactor from the environment and extensive purging of the tubes. The analysis of the products was carried out on an online gas chromatograph (HP 6890 GC) equipped with a flame ionization detector (FID). Separation was performed on a

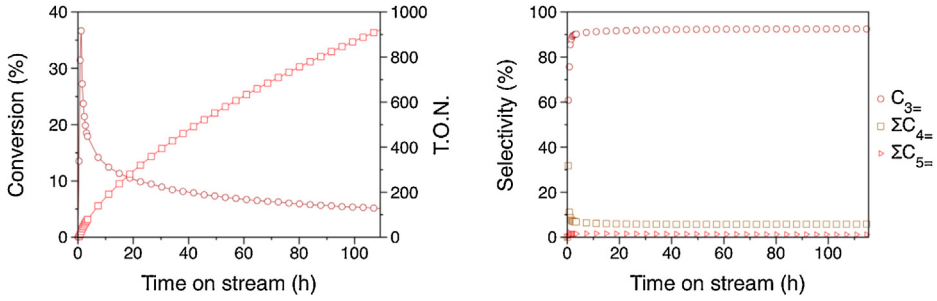

Fig. 1. Conversion of ethylene (○), TON (□) and selectivity *vs.* time on stream.

50 m KCl/Al_2O_3 column. Conversion and selectivity are calculated with respect to the carbon balance.

3. Results and discussion

3.1. Direct conversion of ethylene to propylene over $WH/Al_2O_{3-(500)}$

The catalytic performances of $\mathbf{WH/Al_2O_{3\text{-}(500)}}$, *i.e.* the catalyst prepared from γ-alumina pretreated under vacuum at 500 °C have been tested for the direct conversion of ethylene to propylene. Propylene was obtained selectively (95%) by passing ethylene over $\mathbf{WH/Al_2O_{3-(500)}}$ in a continuous-flow reactor ($P_{C_2H_4} = 1$ bar, $T = 150$ °C, flow rate 4 mL min^{-1} or volume hourly space velocity (VHSV) 400 h^{-1}). The reaction presents an initial steep maximal conversion rate of 0.6 $mol_{C_2H_4}\ mol_W^{-1}\ min^{-1}$ before reaching a pseudo plateau of 0.1 $mol_{C_2H_4}\ mol_W^{-1}\ min^{-1}$ with an overall TON of 930 after 120 h on stream. The selectivity for propylene increases rapidly up to a plateau at 95%, while that of butenes remains below 5% (Fig. 1.). Higher olefins are present in only trace amounts. These results correspond to a productivity of 9.57 $mmol_{C_3H_6}\ g^{-1}\ h^{-1}$ at the maximum and 2.07 $mol_{C_3H_6}\ g^{-1}\ h^{-1}$ at pseudo plateau.

During the 10 first hours on stream, a fast deactivation rate of the catalyst is observed (2.40% h^{-1}), before reaching a pseudo-plateau with a much lower deactivation rate (0.05% h^{-1}). Despite this phenomenon, the selectivity is constant for all catalytic run. A short initiation period is observed in the early stage of catalysis, showing that the tungsten hydride is only the precatalyst of the direct conversion of ethylene to propylene. The initiation step was elucidated by identifying the products formed, in dynamic reactor, while heating to the reaction temperature of 150 °C. Interestingly a non-negligible amount of ethane is observed during the 100 first minutes of catalysis (Fig. S3). About one equivalent of ethane is released per tungsten center after initial contact of $\mathbf{WH/Al_2O_3}$ with ethylene. The reactivity of $\mathbf{WH/Al_2O_{3-(500)}}$ toward ethylene in a batch reactor has also confirmed this equimolar evolution of ethane. This finding suggests the formation of a surface tungsten ethyl-ethylidene species, $[W](CH_2CH_3)(=CHCH_3)$ from tungsten-trisethyl $[W](CH_2CH_3)_3$, by the following elementary steps insertion of three molecules of ethylene into the trishydride, elimination of one ethane by α-H abstraction to form a carbene (Scheme S1). When direct conversion of ethylene to propylene by $\mathbf{WH/Al_2O_{3-(500)}}$ is performed in dynamic reactor, it can be noticed that the conversion is very high (37%) in the early stage of the catalysis. The formation of the active species or ethylene adsorption may also justify this high initial conversion. The mass balance of the reaction has to be studied in order to discriminate the causes of this phenomenon. During the course of the reaction, the mass balance is studied using an ethylene feed with 10% of methane (inert toward $\mathbf{WH/Al_2O_{3-(500)}}$ in these conditions) [34] as internal standard. The ratios of ethylene/methane that come in and out of the reactor toward methane have been plotted (respectively $C_{2=IN}/CH_4$ and $C_{2=OUT}/CH_4$ on Fig. S4). In the same manner, the ratio of products (everything but ethylene) that comes out from the reactor has been plotted ($Products_{OUT}/CH_4$ on Fig. S4). Finally, in order to check if the carbon balance is equilibrated, the sum of $C_{2=OUT}/CH_4$ and $Products_{OUT}/CH_4$ has been plotted (($C_{2=OUT} + Products_{OUT}$)/$CH_4$ on Fig. S3). The result shows that at any time on stream, the carbon balance is equilibrated with respect to the analytical equipment, which implies that at each moment, the mass of gas going in and coming out of the reactor is virtually equal to the mass of ethylene coming in the reactor. Regarding these results it is clear that this high initial activity is due to the catalytic activity and neither to the formation of the active species nor to ethylene adsorption. A first insight into the mechanism of the direct conversion of ethylene to propylene is given by a careful study of the product selectivity at the early stage of the catalysis. Evolution of ethane shows that α-H abstraction leading to the carbenic species occurs only for the first 100 min (Fig. S3). At short time on stream, butene isomers appear in the gas phase. The initial 1-butene/*trans*-2-butene/*cis*-2-butene/isobutene isomeric distribution of 5.2:1:2:3.1 ($t = 20$ min) changed over time, tending to the ratio 1.1:3.2:1:0.7 (Fig. S5). This

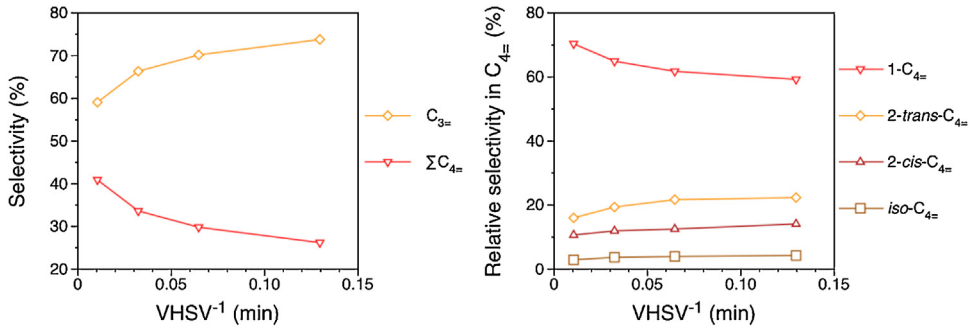

Fig. 2. Global selectivity in propylene and butenes (left) and relative selectivity in butenes (right) *vs.* inverse space velocity at 46 h and 120 °C.

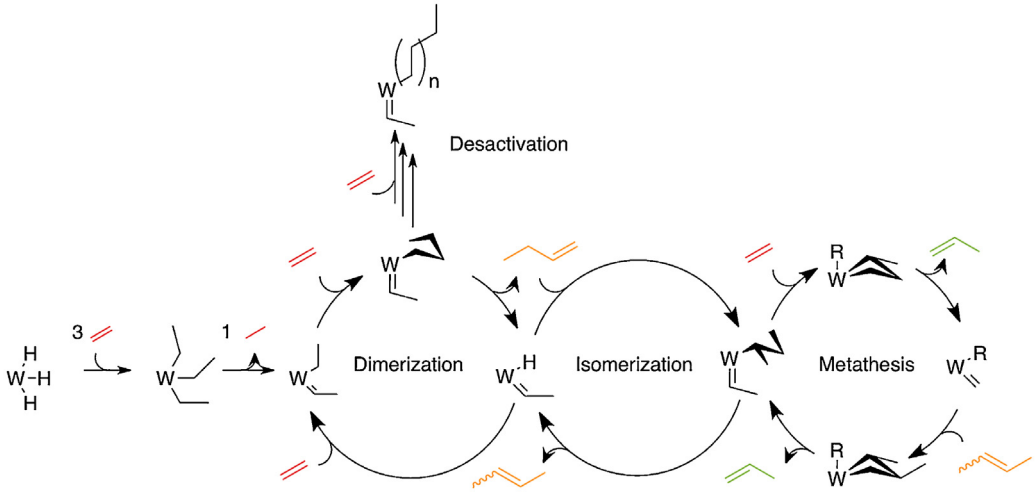

Scheme 2. Global mechanism proposed for the direct conversion of ethylene to propylene on **WH/Al$_2$O$_{3-(500)}$**.

ratio reveals a deficiency of 2-butenes and isobutene compared to the thermodynamic equilibrium values (1:8:3.84:29.6) [35].

In order to understand the propagation mechanism of this reaction, a complete contact time study was performed. The observation of the contact time (VHSV^{-1}) influence on the catalyst performances, *i.e.* conversion and selectivity, reveals two major pieces of information on the catalytic process [36,37]. First, if there is a linear dependence between conversion and contact time that can be extrapolated to zero at zero contact time, it means that the catalytic process is not affected by mass transfer limitations (Fig. S6). The observations can thus be interpreted regarding chemical steps: it is chemical regime. Then, the extrapolated selectivities at zero contact time allow a reliable determination of real primary products. Therefore the reduction of contact time decreases the period when reagents and active sites can interact, reducing *de facto* the formation of secondary products. It has earlier been observed that the selectivity in propylene is constant with time on stream, whereas the deactivation rate is high in the early stage of the catalysis before reaching a pseudo-plateau. To determine if the mechanism of the reaction is the same during these two periods, contact time studies were performed for different time on stream. Thus four experiments of 46 h were carried out at different contact times (Table S1). Plotting the conversion *vs.* inverse space velocity (Fig. S6) confirms that the chemical regime is maintained, whatever the time on stream, in the range of VHSV studied. At each time on stream there is a strong linear dependence, which can be extrapolated to a zero conversion at infinite VHSV, between conversion and contact time. The selectivities observed during these contact time studies (Fig. S7) indicate that butenes are primary products, since the selectivity intercept with the *y*-axis extrapolates to a non-zero value, and that propene is formed in a reaction that consumes butenes, since their curves are mirror images at any flow rate. Furthermore, according to relative selectivity of butene at 46 h on stream *vs.* inverse space velocity (Fig. S8), the formation of 1-butene also appears to precede that of other butenes since it is the only one for which the selectivity increases with decreasing inverse space velocity. It is notable that whatever the time on stream, the global selectivity and butenes partial selectivities *vs.* VHSV^{-1} have the same profiles. Indeed, the mechanism of the conversion of ethylene to propylene stays the same regardless of deactivation of the catalyst. Note that the selectivity in butenes is less than 20% at 150 °C even at low contact time. In order to clarify the fact that 1-butene is the primary product, a study at lower temperature has been performed since the conversion of ethylene/2-butene cross metathesis reaction on **WH/Al$_2$O$_{3-(500)}$** decreases with temperature [27]. To corroborate this hypothesis a contact time study at lower temperature, *i.e.* 120 °C has been performed. The dimerization and metathesis reaction kinetics do not have the same dependency on temperature. The global selectivity in propylene and butenes *vs.* inverse space velocity at 46 h at 120 °C and 150 °C (Figs. 2 and S7) show that higher selectivity in butenes is observed when lowering the reaction temperature (42% at 120 °C *vs.* 16% at 150 °C). Moreover, butenes selectivity clearly increases when contact time decreases (Fig. 2, left). Evidently, at 120 °C these butenes are less consumed by the cross-metathesis reaction than at 150 °C which is less favored by the lower temperature.

These results show that 1-butene is the primary product of the conversion of ethylene to propylene (Fig. 2 right). Its formation occurs by ethylene dimerization by the insertion of two ethylene molecules in the tungsten hydride bond followed by a β-H elimination according to the classical Cosse-Arlman mechanism [38,39]. Then *cis*- and *trans*-2-butenes are obtained after reinsertion of the newly formed 1-butene followed by a second β-H elimination of the sec-butyl species as proposed by Tolman for the isomerization of 1-butene to 2-butene by nickel hydride [40]. Regarding these results, the dimerization seems to be very slow and is the rate-determining step, compared to other reaction occurring further, as it is very difficult to observe 100% selectivity in 1-butene. According to numerous examples [41], olefin cross-metathesis is expected to be catalyzed by a tungsten-alkylidene species following a classical Chauvin mechanism [42]. Furthermore, tungsten alkyl or hydride species also catalyze the isomerization of 1-butene into 2-butenes. Thus, [W](CH$_2$CH$_3$)(=CHCH$_3$), which bears both an alkyl and an alkylidene fragment, is able to catalyze the dimerization, isomerization, and metathesis of olefins on the same site. In other words, it behaves as a trifunctional catalyst (Scheme 2). These multiple functionalities are observed in other reactions carried out by this catalyst such as alkane metathesis [32,43], and conversion of 1-butene or 2-butene to propylene [28,44].

Although the supported tungsten hydride precursor catalyzes an important reaction for propylene production from ethylene feed, it undergoes a significant decrease of activity with time. The deactivation of this catalyst can have different origins: reduction of the tungsten center and/or blocking of active sites by coke or polymers, as reported for different supported olefin metathesis catalysts. Two strategies will be used. The first one consists in the analysis of by-products during ethylene conversion in a continuous flow reactor. The second one is a study of the catalyst at a molecular level by *ex situ* studies by solid state NMR spectroscopy, EPR, UV–vis, DRIFT, TGA and DSC of the used catalyst.

On-stream deactivation during conversion of ethylene to propylene over tungsten hydride catalyst was examined by online analysis of the products. Besides the expected products (according to the previously proposed mechanism), a small amount of isobutene (3%) is also observed. As presented on Scheme S3, the isobutene may have two origins after decomposition of metallacyclobutane by β-H transfer [45]: (i) a "productive" path, where ethylene inserts in the alkyl-hydrido-isobutenyl-tungsten species, then retrieves the active species by α-hydride abstraction; (ii) a "destructive" path, eliminating the isobutyl and hydride ligands followed by reducing the $W^{(VI)}$ to inactive $W^{(IV)}$ as already described for group 6 imido complexes [45,46]. The number of moles of isobutene produced per number of moles of tungsten was calculated and then the cumulated TON $_{isoC4=}$ was plotted *vs.* time on stream. Fig. S9 clearly shows that the production of isobutene is catalytic. After 2 h on stream, the cumulated $TON_{isoC4=}$ exceed 1. Indeed path (i) must occur during the reaction (Scheme S2). Nevertheless, path (ii) may also occur simultaneously. Spectroscopic studies (EPR and UV–Vis) may probe a change of the oxidation state of the used catalyst and thereby provide information about the evolution of the catalyst. It has been well accepted and proved that olefin metathesis reaction occurs on the transitional metal center and follows the metal carbene mechanism [47]. The oxidation state of metal species plays an important role in the metathesis activity [45,48]. Here UV–vis and EPR spectra are applied to detect the oxidation state changes of aged tungsten catalyst.

In fact, at the end of the catalysis no significant color changes were observed. UV–Vis analysis of the fresh W-H/$Al_2O_{3(500)}$ catalyst precursor shows an absorption band at 222 nm, which corresponds to typically W(VI) species (Fig. S10) [49]. The used catalyst has a similar UV–Vis profile with minor red-shift (10 nm), suggesting that the degree of the oxidation state of tungsten remains essentially unchanged after the 260 h on stream. Importantly, no bands corresponding to W(IV) or W(V) species were observed [50]. Moreover, fresh and used catalysts are EPR silent, which further indicate the absent of reduced tungsten species.

^{13}C CP/MAS NMR spectroscopy is an efficient tool to study the nature of the carbonaceous species on aged catalysts [51]. ^{13}C CP/MAS NMR spectrum in Fig. 3 indicates that two broad peaks centered around 32 ppm and 30 ppm are observed, corresponding to respectively crystallized and amorphous PE [52]. No peaks could be observed in the aromatic and olefinic region indicating the carbonaceous deposits are mainly paraffins [27].

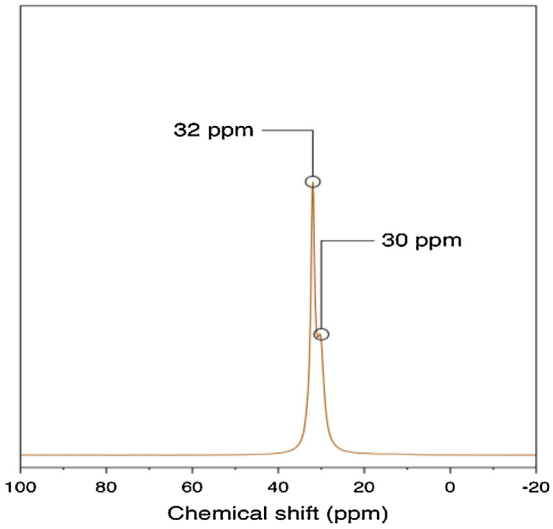

Fig. 3. ^{13}C CPMAS NMR spectrum of the catalyst after 120 h on stream.

In order to better understand the mechanism of deactivation of the catalyst during the direct conversion of ethylene to propylene four experiments have been done in the same conditions ($P_{C_2H_4} = 1$ bar, $T = 150\,^{\circ}C$, flow rate 4 mL min^{-1} or volume hourly space velocity (VHSV) 400 h^{-1}) with different running time (2 h, 24 h, 48 h and 264 h). At the end of each experiment, the catalyst was recovered in the glove box to be analyzed under inert conditions. The study of the aged catalyst was also performed using DRIFT spectroscopy. The DRIFT spectrum (Fig. 4) of the fresh catalyst **WH/$Al_2O_{3-(500)}$** exhibits bands at 3500–3800 cm^{-1}, 2750–3000 cm^{-1}, 1360–1465 cm^{-1} corresponding to $\nu_{(OH)}$ from alumina, $\nu_{(CH)}$ and $\delta_{(CH)}$ from residual hydrocarbon, respectively. Finally the $\nu_{(WH)}$ band is present at 1913 cm^{-1} [32]. The DRIFT spectrum of the used catalyst after 2 h on stream shows a complete disappearance of the $\nu_{(WH)}$ mode, indicating that all the W-H have been inserted by alkenes. Simultaneously, three new bands centered at 2923 cm^{-1}, 2852 cm^{-1} and 1465 cm^{-1} corresponding

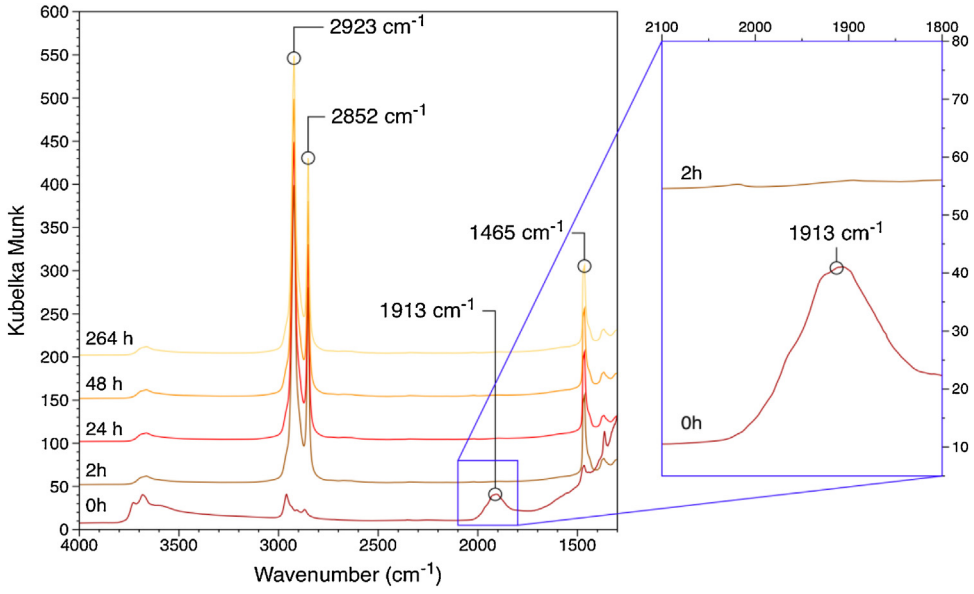

Fig. 4. DRIFT spectra of the fresh catalyst and of the catalytic bed at different time on stream.

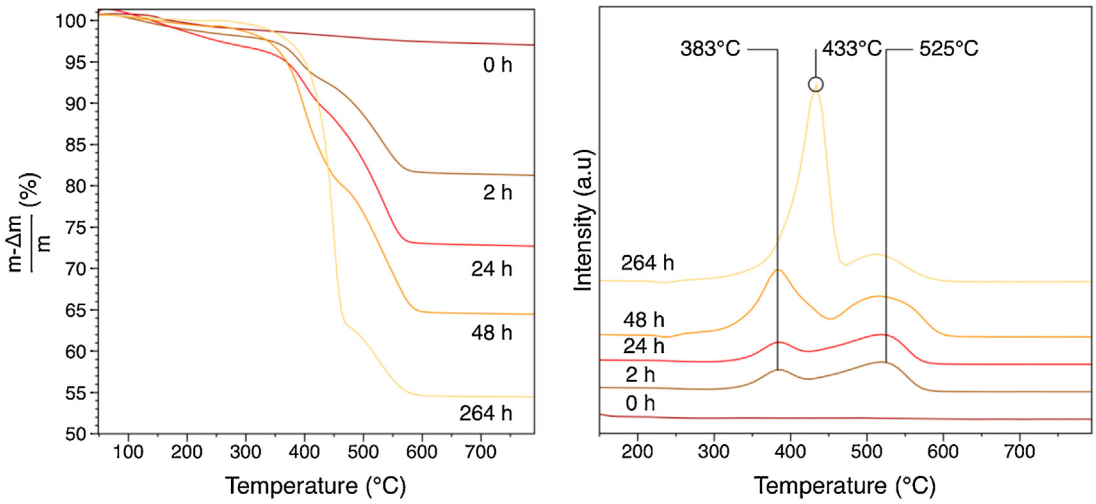

Fig. 5. Left: TGA profiles of the catalyst for each time on stream; right: Differential thermo-gravimetric profiles of the catalyst for each time on stream.

to typical $\nu_{(CH)}$ and $\delta_{(CH)}$ absorptions for long chain alkyl were growing with time on stream. This spectrum is similar to polyethylene obtained by polymerization of ethylene on supported metal hydrides [53].

In order to confirm the hypothesis of the formation of PE, the catalyst was analyzed by TGA and DSC during the direct conversion of ethylene to propylene and compared to the fresh catalyst. The TG profiles, realized under oxidative condition, of the catalysts after given time on stream at 150 °C are presented on Fig. 5. The different weight-loss stages can be seen in the changes in slope of the TG curve and in the maxima of the differential thermo-gravimetric (DTG) profiles. Fig. 5 (right) shows that two main different weight losses are observed: a first between 383 °C and 433 °C and a second around 525 °C. After 2 h, there is 17% of weight loss when the catalyst is completely calcinated, showing a fast formation of surface carbonaceous species on the surface of the catalyst, even at short time on stream. The amount of carbonaceous species gradually increases to reach 46% after 264 h on stream. It clearly indicates that carbonaceous species are formed at the surface of the catalyst during reaction. It is interesting to note on the DTG profiles that at high time on stream, 264 h, the first weight loss peak shifts to 433 °C indicating that the carbonaceous species burns 50 °C higher. In other word, the longer the time on stream is, the more carbonaceous deposits are observed, the harder they are to burn.

Moreover, DSC profiles for melting and crystallization are presented (Fig. 6). The melting DSC profile shows that the melting

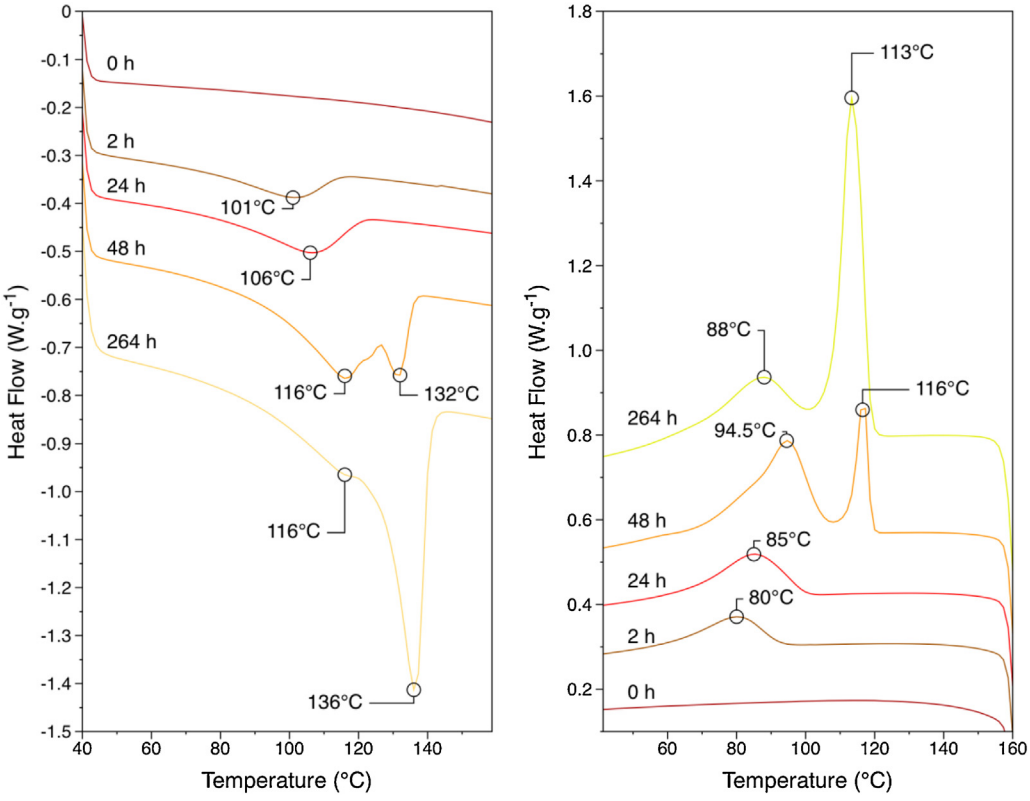

Fig. 6. Left: Fusion DSC profiles for each time on stream; right: crystallization DSC profiles for each time on stream.

peak temperature of the formed species increases with the time on stream: starting at 101 °C after 2 h and reaching 136 °C after 264 h. It is also clear that when the time on stream increases, more than one surface species is formed. This is confirmed by crystallization DSC profiles which show two crystallization peaks after 48 h on stream corresponding to low density PE or heavy PE waxes (*i.e.* species containing more than 60 carbon atoms) [54].

Furthermore, a comparison between the weight loss due to carbonaceous deposits on the used catalyst and the conversion of ethylene (Fig. S11) guide us to the conclusion that the formed carbonaceous products are involved in deactivation. Regarding the last results, it seems that the deactivation of the catalyst is mainly due to the formation of two types of polymers. The drop of initial activity, *i.e.* before 48 h on stream, is accompanied by the formation of a low melting point polymer (116 °C). This polyethylene species may be formed by multiple insertions of ethylene in the supported metal–alkyl bond [55]. The resulting species can then not perform ethylene dimerization anymore, thereby resulting in a deficit of 1-butene, the primary product in the direct conversion of ethylene to propylene. With the low quantity of 1-butene, the overall efficiency of the catalyst drops, therefore leading to the lower conversion levels observed.

The formation of carbonaceous deposits at the surface of the catalyst during metathesis reaction has been observed many times [51,56]. These deposits are assumed to be responsible of the deactivation of the catalyst, such as for WO_3/SiO_2, which is reactivated under air at 500 °C to calcine these deposits and to regenerate the active species [57]. However, contrary to what we have shown here for **$WH/Al_2O_{3-(500)}$**, the industrial catalysts, WO_3/SiO_2 also suffer from deactivation by reduction of the metal center due to the high temperature required for olefin metathesis.

4. Conclusion

The **$WH/Al_2O_{3-(500)}$** catalyst exhibits an outstanding activity in the direct conversion of ethylene to propylene. An extensive contact time study of this reaction shows that 1-butene is the primary product obtained by dimerization of ethylene, the rate determining step for this reaction. The ethylene to propylene mechanism involves a threefold cycle catalyzed by the multifunctional tungsten carbene-hydride moiety supported on alumina: dimerization, isomerization and cross-metathesis. Based on several physical and spectroscopic methods (DRIFT, solid state NMR, EPR, UV–Vis, TGA and DSC), we observed that the active species is deactivated by polymerization with time on stream due to insertion of ethylene into tungsten alkyl groups (Scheme 2) giving low density PE and heavy waxes with a melting point of 116 °C and 136 °C, respectively. Formation of polyethylene also inhibits or prohibits, for at least a fraction of the W sites, the dimerization step (according to the proposed mechanism) and thereby disables turnover of the ethylene to propylene.

Acknowledgment

UOP is acknowledged for generous funding.

Appendix A. Supplementary data

Supplementary material related to this article can be found, in the online version, at http://dx.doi.org/10.1016/j.molcata.2014.01.025.

References

[1] J.S. Plotkin, Catal. Today 106 (2005) 10.
[2] A.H. Tullo, Chem. Eng. News 81 (2003) 15.
[3] K. Fukudome, N.-o. Ikenaga, T. Miyake, T. Suzuki, Catal. Sci. Technol. 1 (2011) 987.
[4] B.V. Vora, Top. Catal. 55 (2012) 1297.
[5] K.C. Szeto, B. Loges, N. Merle, N. Popoff, A. Quadrelli, H. Jia, E. Berrier, A. De Mallmann, L. Deleyoye, R.M. Gauvin, M. Taoufik, Organometallics 32 (2013) 6452.
[6] P. Amigues, Y. Chauvin, D. Commereuc, C.T. Hong, C.C. Lai, Y.H. Liu, J. Mol. Catal. 65 (1991) 39.
[7] T.I. Bhuiyan, P. Arudra, M.N. Akhtar, A.M. Aitani, R.H. Abudawoud, M.A. Al-Yami, S.S. Al-Khattaf, Appl. Catal., A 467 (2013) 224.
[8] D.R. Hua, S.L. Chen, G.M. Yuan, Y.L. Wang, Q.F. Zhao, X.L. Wang, B. Fu, Microporous Mesoporous Mater. 143 (2011) 320.
[9] H.J. Liu, L. Zhang, X.J. Li, S.J. Huang, S.L. Liu, W.J. Xin, S.J. Xie, L.Y. Xu, J. Nat. Gas Chem.V 18 (2009) 331.
[10] J.C. Mol, J. Mol. Catal. A: Chem. 213 (2004) 39.
[11] D.Z. Zhang, X.J. Li, S.L. Liu, S.J. Huang, X.X. Zhu, F.C. Chen, S.J. Xie, L.Y. Xu, Appl. Catal., A 439 (2012) 171.
[12] S. Ilias, A. Bhan, ACS Catal. 3 (2013) 18.
[13] D.M. McCann, D. Lesthaeghe, P.W. Kletnieks, D.R. Guenther, M.J. Hayman, V. Van Speybroeck, M. Waroquier, J.F. Haw, Angew. Chem. Int. Ed. 47 (2008) 5179.
[14] J. He, T. Xu, Z. Wang, Q. Zhang, W. Deng, Y. Wang, Angew. Chem. Int. Ed. 51 (2012) 2438.
[15] M.H. Nilsen, S. Svelle, S. Aravinthan, U. Olsbye, Appl. Catal., A 367 (2009) 23.
[16] U. Olsbye, O.V. Saure, N.B. Muddada, S. Bordiga, C. Lamberti, M.H. Nilsen, K.P. Lillerud, S. Svelle, Catal. Today 171 (2011) 211.
[17] A.H. Tullo, J. Johnson, Chem. Eng. News 91 (2013) 9.
[18] P.P. Oneill, J.J. Rooney, J. Am. Chem. Soc. 94 (1972) 4383.
[19] F. Hugues, B. Besson, J.M. Basset, J. Chem. Soc., Chem. Commun. (1980) 719.
[20] H. Imamura, T. Konishi, Lanthanide Actinide Res. 3 (1991) 387.
[21] T. Yamaguchi, Y. Tanaka, K. Tanabe, J. Catal. 65 (1980) 442.
[22] T. Suzuki, K. Tanaka, I. Toyoshima, H. Gotoh, Appl. Catal. 50 (1989) 15.
[23] T. Suzuki, React. Kinet. Catal. Lett. 81 (2004) 327.
[24] H. Oikawa, Y. Shibata, K. Inazu, Y. Iwase, K. Murai, S. Hyodo, G. Kobayashi, T. Baba, Appl. Catal., A 312 (2006) 181.
[25] M. Iwamoto, Catal. Surv. Asia 12 (2008) 28.
[26] M. Iwamoto, Y. Kosugi, J. Phys. Chem. C 111 (2007) 13.
[27] E. Mazoyer, K.C. Szeto, N. Merle, S. Norsic, O. Boyron, J.-M. Basset, M. Taoufik, C.P. Nicholas, J. Catal. 301 (2013) 1.
[28] E. Mazoyer, K.C. Szeto, J.-M. Basset, C.P. Nicholas, M. Taoufik, Chem. Commun. 48 (2012) 3611.
[29] M. Taoufik, E. Le Roux, J. Thivolle-Cazat, J.-M. Basset, Angew. Chem. Int. Ed. 46 (2007) 7202.
[30] N. Popoff, E. Mazoyer, J. Pelletier, R.M. Gauvin, M. Taoufik, Chem. Soc. Rev. 42 (2013) 9035.
[31] K.C. Szeto, E. Mazoyer, N. Merle, S. Norsic, J.M. Basset, C.P. Nicholas, M. Taoufik, ACS Catal. 3 (2013) 2162.
[32] E. Le Roux, M. Taoufik, C. Coperet, A. de Mallmann, J. Thivolle-Cazat, J.M. Basset, B.M. Maunders, G.J. Sunley, Angew. Chem. Int. Ed. 44 (2005) 6755.
[33] D.N. Clark, R.R. Schrock, J. Am. Chem. Soc. 100 (1978) 6774.
[34] K.C. Szeto, S. Norsic, L. Hardou, E. Le Roux, S. Chakka, J. Thivolle-Cazat, A. Baudouin, C. Papaioannou, J.M. Basset, M. Taoufik, Chem. Commun. 46 (2010) 3985.
[35] R.A. Alberty, C.A. Gehrig, J. Phys. Chem. Ref. Data 14 (1985) 803.
[36] R.A. van Santen, J.A. Moulijn, P.W.N.M. van Leeuwen, B.A. Averill, Catalysis: An Integrated Approach, Elsevier, Amsterdam, 1999.
[37] J.M. Basset, C. Coperet, L. Lefort, B.M. Maunders, O. Maury, E. Le Roux, G. Saggio, S. Soignier, D. Soulivong, G.J. Sunley, M. Taoufik, J. Thivolle-Cazat, J. Am. Chem. Soc. 127 (2005) 8604.
[38] E.J. Arlman, P. Cossee, J. Catal. 3 (1964) 99.
[39] P. Cossee, J. Catal. 3 (1964) 80.
[40] C.A. Tolman, J. Am. Chem. Soc. 94 (1972) 2994.
[41] K.J. Ivin, J.C. Mol, Olefin Metathesis and Metathesis Polymerization, Academic Press, San Diego, CA, 1997.
[42] J.L. Herisson, Y. Chauvin, Makromol. Chem. 141 (1971) 161.
[43] K.C. Szeto, L. Hardou, N. Merle, J.-M. Basset, J. Thivolle-Cazat, C. Papaioannou, M. Taoufik, Catal. Sci. Technol. 2 (2012) 1336.
[44] E. Mazoyer, K.C. Szeto, S. Norsic, A. Garron, J.-M. Basset, C.P. Nicholas, M. Taoufik, ACS Catal. 1 (2011) 1643.
[45] J. Robbins, G.C. Bazan, J.S. Murdzek, M.B. Oregan, R.R. Schrock, Organometallics 10 (1991) 2902.
[46] E. Mazoyer, N. Merle, A. de Mallmann, J.-M. Basset, E. Berrier, L. Delevoye, J.-F. Paul, C.P. Nicholas, R.M. Gauvin, M. Taoufik, Chem. Commun. 46 (2010) 8944.
[47] M. Jezequel, V. Dufaud, M.J. Ruiz-Garcia, F. Carrillo-Hermosilla, U. Neugebauer, G.P. Niccolai, F. Lefebvre, F. Bayard, J. Corker, S. Fiddy, J. Evans, J.P. Broyer, J. Malinge, J.M. Basset, J. Am. Chem. Soc. 123 (2001) 3520.
[48] H. Ahn, T.J. Marks, J. Am. Chem. Soc. 124 (2002) 7103.
[49] E.I. Ross-Medgaarden, I.E. Wachs, J. Phys. Chem. C 111 (2007) 15089.
[50] G.A. Ozin, R.A. Prokopowicz, S. Ozkar, J. Am. Chem. Soc. 114 (1992) 8953.

[51] X. Li, W. Zhang, X. Li, S. Liu, H. Huang, X. Han, L. Xu, X. Bao, J. Phys. Chem. C. 113 (2009) 8228.
[52] G. Nowaczyk, S. Glowinkowski, S. Jurga, Solid State Nucl. Magn. Reson. 25 (2004) 194.
[53] G. Tosin, C.C. Santini, J.-M. Basset, Top. Catal. 52 (2009) 1203.
[54] Y. Chen, H. Zou, M. Liang, P. Liu, J. Appl. Polym. Sci. 129 (2013) 945.
[55] J.M. Basset, R. Psaro, D. Roberto, R. Ugo, Modern Surface Organometallic Chemistry, Wiley-VCH, Weinheim, 2009.
[56] A. Spamer, T.I. Dube, D.J. Moodley, C. van Schalkwyk, J.M. Botha, Appl. Catal., A 255 (2003) 133.
[57] C. van Schalkwyk, A. Spamer, D.J. Moodley, T. Dube, J. Reynhardt, J.M. Botha, Appl. Catal., A 255 (2003) 121.